Design of 6.6 kV, 100 A saturated DC reactor type superconducting fault current limiter

AUTHOR(S):

Hoshino, T; Salim, KM; Kawasaki, A; Muta, I; Nakamura, T; Yamada, M

CITATION:

Hoshino, T ...[et al]. Design of 6.6 kV, 100 A saturated DC reactor type superconducting fault current limiter. IEEE TRANSACTIONS ON APPLIED SUPERCONDUCTIVITY 2003, 13(2): 2012-2015

ISSUE DATE:

2003-06

URL:

http://hdl.handle.net/2433/39948

Design of 6.6 kV, 100 A Saturated DC Reactor Type Superconducting Fault Current Limiter

Tsutomu Hoshino, Khosru Mohammad Salim, Akio Kawasaki, Itsuya Muta, *Member, IEEE*, Taketsune Nakamura, and Masato Yamada

***Abstract*—Proposed saturated DC reactor type superconducting fault current limiter (SFCL) was designed and fabricated. The rated value was 100 V and 10 A for small scale experiment. The relationships between the one-turn voltage and the cross section of the core, the inductance value are obtained. The optimized cross section of the core was 90 mm × 45 mm under restriction of the core manufacturer. The core material was ultra fine grain steel named FINEMET® FT-3H. The number of main winding was 100 turn and that of control winding was also 100 turn. The wires are NbTi superconductor with different filament diameter. We enhanced this design scheme to 6.6 kV, 100 A SFCL. The core cross section size and core gap and core length of 6.6 kV design are presented.**

***Index Terms*—DC reactor, fault current limiter, material, soft magnet, superconductor.**

I. Introduction

PROPOSED saturated DC reactor type superconducting fault current limiter (SFCL) [1] is classified as one of bridge type SFCL [2], [3] which will operate as circuit breaker [4] with the gate signal control of the thyristor. Any semiconductor device has absolute rated current. The current through the device should be restricted less than its rated current. The semiconductor circuit breaker (CB) will requires proper current limiting mechanism. Bridge type SFCL has an advantage on recovery to normal operation. Using superconductivity state to normal-conductivity state phase transition (SN transition), such as superconducting transformer with auxiliary winding [5], [6] and noninductive reactor type SFCL [7], [8] have problem to recover superconducting state, i.e., normal operation. In the series connected resistive type SFCL has also problem [9].

We have pointed out that a rectifying type SFCL without DC bias source in main circuit shows unexpected limiting performance when load current increases abruptly [1]. We have shown the solution of this problem by using saturated DC reactor, and fabricated a small scale of 100 V, 10 A SFCL and made some experiments. In this paper, we propose design of 6.6 kV, 100 A saturated DC reactor type SFCL.

Manuscript received August 6, 2002. This work was supported in part by The Kansai Electric Power Company, Inc.

T. Hoshino, K. M. Salim, A. Kawasaki, I. Muta, and T. Nakamura are with the Graduate School of Engineering, Kyoto University, Kyoto 606-8501, Japan (e-mail: hoshino@kuee.kyoto-u.ac.jp; muta@kuee.kyoto-u.ac.jp; tk_naka@kuee.kyoto-u.ac.jp; khosru@audrey.kuee.kyoto-u.ac.jp; kawasaki@audrey.kuee.kyoto-u.ac.jp).

M. Yamada is with General R&D Center, Kansai Electric Power Co., Hyogo 661-0974, Japan (e-mail: K431639@kepco.co.jp).

Digital Object Identifier 10.1109/TASC.2003.812967

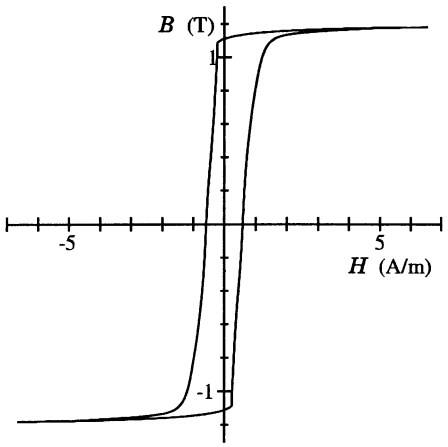

Fig. 1. Measured B–H curve of FT-3H, at $f = 40$ mHz, $A_e = 299.7$ mm^2, $l_e = 321.4$ mm, $H_c = 0.6$ A/m, $B_{ms} = 1.23$ T at 800 A/m.

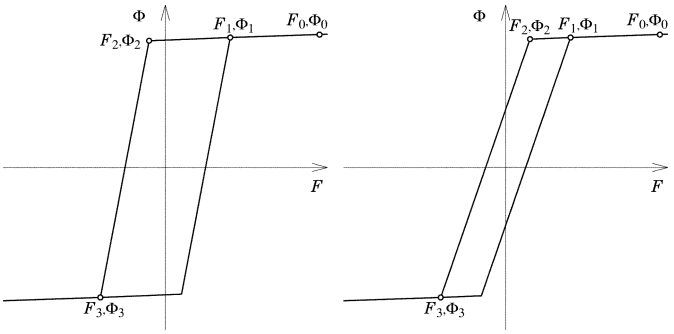

Fig. 2. The idealized relationship between magnetomotive force F and magnetic flux Φ. (a) FINEMET® FT-3H for the small model [11]. (b) FINEMET® FT-3L.

II. Magnetic Property for Analysis

Hitachi Metals developed a new soft magnetic material (so called FINEMET®) [10] that uses super-sudden cooling technology. This ferrite-based alloy consisting of nanocrystalline particles is an epoch-making new material with high saturation flux density and low magnetostriction.

FINEMET® FT-3H was selected as the iron core material because of low loss, magnetic properties of high rectangular and zero magnetostriction. The measured B–H curve of FT-3H for the 100 V, 10 A class small scale model [11] is shown in Fig. 1. The idealized relationship between magnetomotive force (mmf) F and magnetic flux Φ was represented by combination

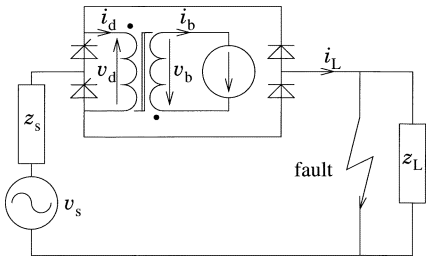

Fig. 3. Circuit diagram with saturated DC reactor type SFCL.

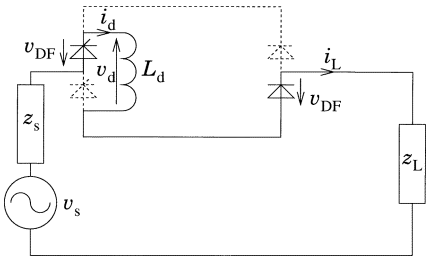

Fig. 4. Circuit diagram at charging mode of reactor.

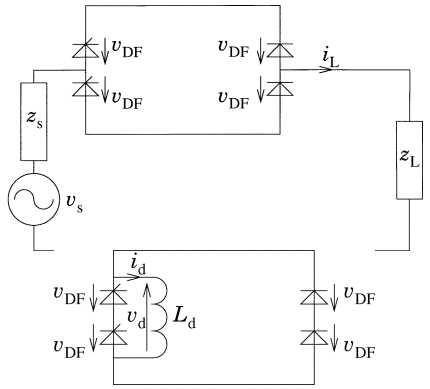

Fig. 5. Circuit diagram at bypass (freewheeling) mode of reactor. (a) Line current circuit, (b) reactor current circuit.

of straight line as shown in Fig. 2(a). Each point means that (F_0, Φ_0) is bias point, (F_1, Φ_1) is saturate point, (F_2, Φ_2) is start point of limiting, and (F_3, Φ_3) is end point of limiting. When N turn winding is wound the core, the differential inductance $L = N(\mathrm{d}\Phi/\mathrm{d}I) = N^2(\mathrm{d}\Phi/\mathrm{d}F)$ is constant except its fold point (F_2, Φ_2). This assumption brings simplification of the analysis. And the flux between thin layer tape of the core material is negligible small (less than 0.1% of flux in the core), and the leakage flux is also negligible (less than 2.5%). Fig. 2(b) shows idealized $F-\Phi$ curve of FT-3L which has low hysteresis loss and wide mmf range F_2–F_3 for the alternative material for longer limiting duration. The value F_2–F_3 is adjustable by the gap length introduced in the core.

The circuit diagram is shown in Fig. 3. There is a DC current source in the auxiliary circuit named control circuit of the core bias poing. This source is easier implementation compared with the source in main circuit [3]. An operating point of the core changes the total mmf. The principle of our SFCL is changing the operating point of the core by the total mmf. In normal operation, the operating point is set in the saturated region between F_0 and F_2. F_0 corresponds to the mmf which is the product of control current i_b and the turn number of the control winding N_b. Total mmf F is given as $F_0 - Ni_d = N_b i_b - Ni_d$. When fault occurs, the operating point of the core moves to the non-saturated region. When the current through DC reactor winding i_d reached to $I_N = (F_0 - F_2)/N$, high impedance appears in the iron core until the current i_d reached to $I_S = (F_0 - F_3)/N$. In the case of $i_d > I_s$, the operating point of the core enters saturated region again. The inductance of the DC reactor is described as follows:

$$L_d = \begin{cases} L_S = N^2 \dfrac{\phi_0 - \phi_1}{F_0 - F_1} = N^2 \mu_s \dfrac{A_e}{l_e} \\ L_N = N^2 \dfrac{\phi_2 - \phi_3}{F_2 - F_3} = N^2 \mu_n \dfrac{A_e}{l_e} \end{cases} \tag{1}$$

where $\Delta F = \Delta H l_e$, $\Delta\Phi = \Delta B A_e$, A_e is effective magnetic cross section area, l_e is effective magnetic length, μ_s is differential permeability of saturated region and μ_n is the one of non-saturated region, respectively. And L_s and L_n is inductance in saturated region and nonsaturated region, respectively.

III. Circuit Diagram and Analysis

To simplify the circuit analysis for the design, the concentrated constant was used. The load impedance is connected to the voltage source through saturated DC reactor type superconducting fault current limiter as shown in Fig. 3. The inductive source impedance $\dot{z}_s = r_s + \mathrm{j}\omega L_s$ was assumed. The fault point was taken at the terminal of the load side of SFCL. The load impedance $\dot{z}_L = r_L + \mathrm{j}\omega x_L$ includes line impedance and Lagging load. In this paper, lagging power factor was discussed for simplification.

The circuit operation is classified into two mode. The first mode is exciting mode of the DC reactor L_d as shown in Fig. 4. The line current i_L flows the solid line path or the broken line path according to the current direction. This mode begins at $t = t_0$ and ends at $t = t_1$, T denotes voltage source period ($\omega T = 2\pi$). $(n-1)T/2 < t_0 < t_1 < nT/2$. The circuit equation is given as follows:

$$\sqrt{2}V \sin\omega t = ri + \frac{\mathrm{d}Li}{\mathrm{d}t} - (-1)^n 2v_{DF} \tag{2}$$

where $i = (-1)^{n-1} i_d = i_L$, $r = r_s + r_L$ is equivalent resistance, $L = L_s + L_d + L_L$ is equivalent inductance, and v_{DF} assumed to constant is the forward voltage drop of the diode and the thyristor. Though all semiconductor devices are on state, the constant forward voltage drop $v_{DF} \simeq V_{DF}$ is assumed. The current i is described as follows:

$$i = e^{-(r/L)(t-t_0)} \left\{ i_0 - \frac{\sqrt{2}V}{z} \sin(\omega t_0 - \psi) - (-1)^n \frac{2V_{DF}}{r} \right\} + \frac{\sqrt{2}V}{z} \sin(\omega t - \psi) + (-1)^n \frac{2V_{DF}}{r} \tag{3}$$

where $i_0 = i(t_0)$, $z = \sqrt{r^2 + (\omega L)^2}$, $\tan\psi = L/r$.

The second mode is freewheeling (bypass SFCL) mode as shown in Fig. 5. The line current i_L flows both the upper and lower path of the bridge as shown Fig. 5(a). The circuit equation is

$$\sqrt{2}V \sin\omega t = ri_L + \frac{\mathrm{d}Li_L}{\mathrm{d}t} \tag{4}$$

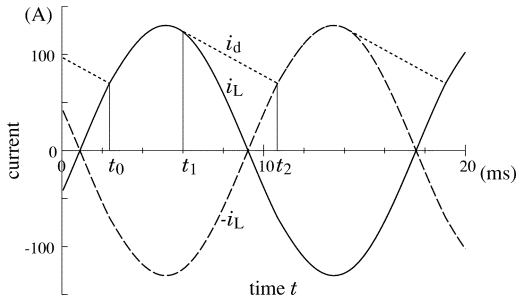

Fig. 6. Current waveform at normal operation, where $V = 6.6$ kV, $f = 60$ Hz, $V_{DF} = 50$ V, $\dot{z}_s = 66.0$ m Ω + j3.30 Ω, $\dot{z}_L = 66.0\,\Omega$ + j19.8 Ω, $L_d = 8.75$ mH.

where $L = L_s + L_L$ is equivalent inductance. The reactor current i_d flows the diode and thyristor. The circuit equation is as follows:

$$\frac{\mathrm{d}L_d i_d}{\mathrm{d}t} = v_{DF} + v_{DF} = 2v_{DF}. \tag{5}$$

This mode begins at $t = t_1 > (n-1)T/2$ and ends at $t = t_2 < nT/2$. The currents i_L and i_d are described as follows:

$$i_L(t) = e^{-(r/L)(t-t_1)}\left\{i_1 - \frac{\sqrt{2}V}{z}\sin(\omega t_1 - \psi)\right\} + \frac{\sqrt{2}V}{z}\sin(\omega t - \psi) \tag{6}$$

$$i_d(t) = i_1 - \frac{\sqrt{2}V_{DF}}{L_d}(t - t_1) \tag{7}$$

where $i_1 = i(t_1) = i_L(t_1) = i_d(t_1)$.

In the steady state (normal operation), the waveform repeats every half cycle, i.e., $t_2 = t_0 + T/2$, and $i_L(t_2) = (-1)^n i_d(t_2)$ as shown in Fig. 6. The inductance of DC reactor was 8.75 mH which is 5% of base inductance ($L_B = 175$ mH). The DC inductance value was set to no voltage-sag condition [12].

When the fault occurs at $t = t_3$, the fault impedance z_f is substituted to the load impedance z_L. In the case $t_1 < t_3 < t_2$, the load current i_L increases sharply bypassing the DC reactor as shown in Fig. 7. The load current reached to the reactor current at $t = t_4$, i.e., $i_L(t_4) = i_d(t_4)$, the DC reactor $L_d = L_s$ limits the fault current slightly. At $t = t_5$, the reactor current reached nonsaturated condition $i_d(t_5) = I_N$, the DC inductance L_d changes its value from L_S to L_N. At $t = t_6$, the reactor current reached again saturated condition $i_d(t_6) = I_S$, the DC inductance L_d changes its value from L_N to L_S. The turn-on signal should be shutdown before the time t_6 to protect lines and equipment as a circuit breaker.

For the simplification, we assume $0 < t_5 < T/2$. In the first charging mode

$$i(t) = e^{-(r/L)(t-t_5)}\left\{I_N - \frac{\sqrt{2}V}{z}\sin(\omega t_5 - \psi) + \frac{2V_{DF}}{r}\right\} + \frac{\sqrt{2}V}{z}\sin(\omega t - \psi) - \frac{2V_{DF}}{r} \tag{8}$$

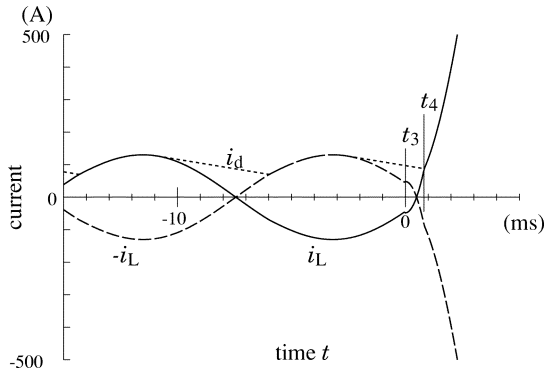

Fig. 7. Current waveform at beginning of fault operation, where $V = 6.6$ kV, $f = 60$ Hz, $V_{DF} = 50$ V, $\dot{z}_s = 66.0$ mΩ + j3.30 Ω, $\dot{z}_f = 10.0$ mΩ + j0 Ω, $L_d = L_S = 8.75$ mH, $T_3 = 0$ ms.

where $r = r_s + r_f$, $L = L_s + L_N + L_f$, $\tan\psi = L/r$ and $z = \sqrt{(r_s + r_f)^2 + \{\omega(L_s + L_d + L_f)\}^2}$. At $t = t_{a1}$, the bypass mode starts, and end at $t = t_{b1}$

$$i_L(t) = e^{-(r/L)(t-t_{a1})}\left\{i_{a1} - \frac{\sqrt{2}V}{z}\sin(\omega t_{a1} - \psi)\right\} + \frac{\sqrt{2}V}{z}\sin(\omega t - \psi) \tag{9}$$

$$i_d(t) = i_{a1} - \frac{\sqrt{2}V_{DF}}{L_d}(t - t_{a1}) \tag{10}$$

where $i_{a1} = i(t_{a1}) = i_L(t_{a1}) = i_d(t_{a1})$. t_{a1} is given by

$$\left.\frac{\mathrm{d}i}{\mathrm{d}t}\right|_{t=t_{a1}} = 0.$$

$$re^{-(r/L)(t_{a1}-t_5)}\left\{I_N - \frac{\sqrt{2}V}{z}\sin(\omega t_5 - \psi) + \frac{2V_{DF}}{r}\right\} = \omega L\frac{\sqrt{2}V}{z}\cos(\omega t_{a1} - \psi). \tag{11}$$

This equation is a transcendental function, the strict solution could not obtained. In the second charging mode

$$i(t) = e^{-(r/L)(t-t_{b1})}\left\{I_{b1} - \frac{\sqrt{2}V}{z}\sin(\omega t_{b1} - \psi) + \frac{2V_{DF}}{r}\right\} + \frac{\sqrt{2}V}{z}\sin(\omega t - \psi) - \frac{2V_{DF}}{r} \tag{12}$$

where $i_{b1} = i(t_{b1}) = i_L(t_{b1}) = -i_d(t_{b1})$.

Instead of solving equation (11), we substitute DC voltage source as shown in Fig. 9. The current $i_d = i_L$ is given as follows:

$$i_d(t) = e^{-(r/L)(t-t_5)}I_N + \left\{1 - e^{-(r/L)(t-t_5)}\right\}\frac{V_{Ds} - 2V_{DF}}{r} \tag{13}$$

where $V_{Ds} = (2\sqrt{2})/(\pi)V$. By the condition of $i_d(t_6) = I_S$,

$$t_6 - t_5 = \frac{L}{r}\ln\frac{rI_S - V_{Ds} + 2V_{DF}}{rI_N - V_{Ds} + 2V_{DF}}. \tag{14}$$

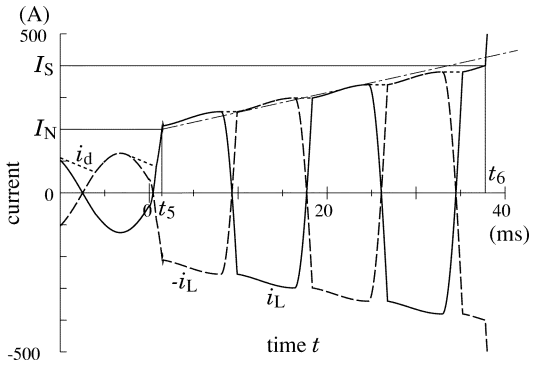

Fig. 8. Current waveform at current limiting mode with increased inductance, where $V = 6.6$ kV, $f = 60$ Hz, $V_{DF} = 50$ V, $\dot{z}_s = 66.0\,\mathrm{m\Omega} + \mathrm{j}3.30\,\Omega$, $\dot{z}_f = 10.0\,\mathrm{m\Omega} + \mathrm{j}0\Omega$, $L_d = L_N = 875$ mH. $I_N = 200$ A, $I_s = 400$ A.

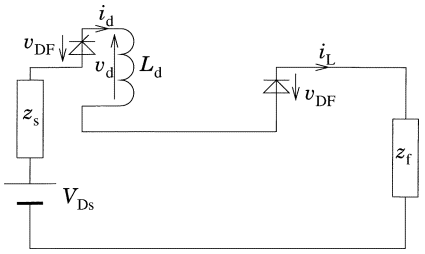

Fig. 9. Alternative circuit diagram at current limiting mode.

The wave form of equation (13) is shown in Fig. 8 as an alternate long and short dash line. When the total resistance r is negligible small, equation (14) is modified as follows:

$$t_6 - t_5 = \frac{L_d + L_s + L_f}{V_{Ds} - 2V_{DF}}(I_S - I_N) \simeq \frac{L_N}{V_{Ds}}(I_S - I_N). \quad (15)$$

If the current limiting interval $t_6 - t_5 = kT$ is set to the k times of the source interval T, the required DC inductance is

$$L_N = kT\frac{V_{Ds}}{I_S - I_N}. \quad (16)$$

IV. Design of 6.6 kV SFCL

We select base current $I_B = 100$ A, $I_N = \alpha I_B$, $I_S = \beta I_B$, $f = 60$ Hz, $V_B = 6.6$ kV, base inductance $L_B = V_B/(2\pi f I_B) = 175$ mH, and $\alpha = 2$, $\beta = 4$. For the FINEMET® FT-3H, $\Delta B = 2.46$ T, $\Delta H = 1.35$ A/m, and for FT-3L, $\Delta B = 2.46$ T, $\Delta H = 24.0$ A/m are given.

Without introducing the gap in the core, following relations are obtained: $L_N/L_B = 4\sqrt{2}k/(\beta - \alpha) \simeq 2.83k$, $NA_e = 2\sqrt{2}kTV_B/(\pi\Delta B) \simeq 40.3k$ m^2, $l_e/N = (I_S - I_N)/\Delta H = (\beta - \alpha)I_B/\Delta H \simeq 148$ m and 8.33 m, for FT-3H and FT-3L, respectively. The relationship between turn voltage and the cross section area A_e is shown in Fig. 10. When the gap l_g is introduced in the core length l_c, the effective length is given as $l_e = l_c + (\Delta B/\mu_0\Delta H)l_g \simeq (\Delta B/\mu_0\Delta H)l_g$. The required gap length is $l_g/N = \mu_0(\beta - \alpha)I_B/\Delta B \simeq 0.102$ mm. In the case of $k = 1$ and $N = 400$, the parameters $A_e = 0.1$ m^2 and $l_g = 40$ mm were obtained . If the window size is 30 cm $\times$ 60 cm, the core length $l_c \simeq 3$ m.

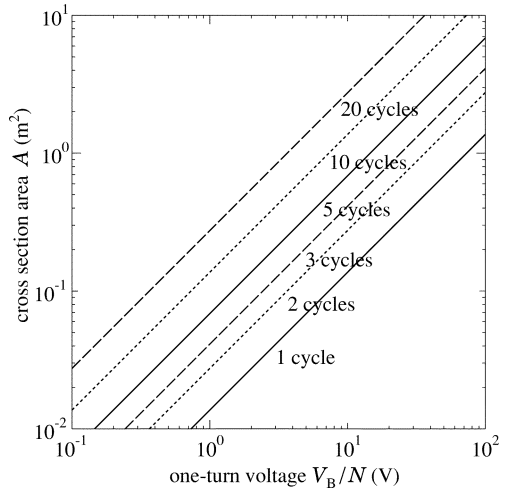

Fig. 10. The relationship between turn voltage and the cross section area of the FINEMET® FT-3H.

V. Conclusion

We have analyzed the circuit equations of the saturated DC reactor type SFCL, and get the relationship between one turn voltage and core cross section. For 6.6 kV, 100 A rated SFCL, the effective core cross section area, the effective core length and the gap length were obtained. Those dimensions are acceptable.

References

[1] T. Hoshino, K. M. Salim, M. Nishikawa, I. Muta, and T. Nakamura, "Proposal of saturated DC reactor type superconducting fault current limiter (SFCL)," *Cryogenics*, vol. 41, pp. 469–474, July 2001.

[2] H. J. Boening and D. A. Paice, "Fault current limiter using superconducting coil," *IEEE Trans. Magn.*, vol. MAG-19, pp. 1051–1053, May 1983.

[3] T. Ishigohka, A. Ninomiya, and Y. Kuwamura, "Fabrication and test of cryogenic fault current limiter combining semiconductors and DC reactor," in *Proc. IPEC-Tokyo 2000*, vol. 3, Apr. 2000, pp. 1525–1528.

[4] T. Ueda *et al.*, "Solid-state current limiter for power distribution system," *IEEE Trans. Power Delivery*, vol. 8, pp. 1796–1801, Oct. 1993.

[5] I. Muta, Y. Morita, T. Hoshino, and K. Ogura, "Preliminary study on superconducting transformer and fault current limiting devices for electric power system," in *Proc. China Int. Conf. Electrical Machines*, 1991, pp. 12–15.

[6] T. Hoshino and I. Muta, "Load test on superconducting transformer and fault current limiting devices for electric power system," *IEEE Trans. Magn.*, vol. 30, no. 4, pp. 2018–2021, 1994.

[7] T. Hoshino, I. Muta, and M. Baba, "Preliminary study on noninductive reactor type fault current limiter," *Cryogenics*, vol. 34, pp. 753–756, 1994.

[8] T. Hoshino, I. Muta, H. Tsukiji, K. Ohkubo, and M. Etoh, "Recovery time of superconducting noninductive reactor type fault current limiter," *IEEE Trans. Magn.*, vol. 32, no. 4, pp. 2403–2406, 1996.

[9] T. Hoshino, M. Nishikawa, K. M. Salim, T. Nakamura, and I. Muta, "Preliminary studies on characteristics of series-connected resistive type superconducting fault current limiter for system design," *Physica C*, vol. 354, no. 1–4, pp. 120–124, May 2001.

[10] K. Hono, K. Hiraga, Q. Wang, A. Inoue, and T. Sakurai, "The microstructure evolution of a $Fe_{73.5}Si_{13.5}B_9Nb_3CU_1$ nanocrystalline soft magnetic material," *Acta Metall. Mater.*, vol. 40, pp. 2137–2147, Sept. 1992.

[11] K. M. Salim, T. Hoshino, M. Nishikawa, I. Muta, and T. Nakamura, "Preliminary experiments on saturated DC reactor type fault current limiter," *IEEE Trans. Appl. Superconduct.*, vol. 12, pp. 872–875, Mar. 2002.

[12] K. M. Salim, T. Hoshino, A. Kawasaki, I. Muta, and T. Nakamura, "Waveform analysis of the Bridge type SFCL considering load changing and fault time," in *Applied Superconductivity Conf.*, Houston, TX, Aug. 2002, 2LE01, pp. 4–9.